Inorganic Chemistry

Article

pubs.acs.org/IC

Slow Magnetic Relaxation Observed in Dysprosium Compounds Containing Unsupported Near-Linear Hydroxo- and Fluoro-Bridges

Gabriel Brunet, Fatemah Habib, Ilia Korobkov, and Muralee Murugesu*

Department of Chemistry, University of Ottawa, 10 Marie-Curie, Ottawa, Ontario K1N 6N5, Canada

Supporting Information

ABSTRACT: The encapsulating *N*1,*N*3-bis(3-methoxysalicylidene)diethylenetriamine (H_2valdien) ligand was employed to isolate two novel Dy^{III} compounds which contain rare bridging pathways for lanthanide systems. Compound **1**, $[Na_2Dy^{III}{}_2(valdien)_2(\mu\text{-}OH)(dbm)_2(H_2O)_2][Na_2Dy^{III}{}_2(valdien)_2(\mu\text{-}OH)(NO_3)_2(dbm)_2]$, where dbm^- is dibenzoylmethanido, and compound **2**, $[Na_3Dy^{III}{}_2(valdien)_2(\mu\text{-}F)(\mu_3\text{-}F)_2(Cl)_2(MeOH)_2]_n \cdot 0.5(MeOH)\cdot(H_2O)$, both exhibit linear lone hydroxo- and fluoro-bridges, respectively, between the metal centers. The unit cell of **1** comprises two discrete dinuclear molecules, which differ slightly, forming a cation−anion pair, while **2** forms a coordination polymer. The magnetic investigations indicate that both compounds display ferromagnetic coupling between the Dy^{III} ions. Magnetic susceptibility measurements in the temperature range 1.8−300 K reveal that the Dy^{III} ions in **1** are weakly coupled, resulting in a mononuclear single-molecule magnet-like behavior under an applied field. In the case of **2**, the stronger coupling arising from the fluoride-bridge, leads to zero-field single-molecule magnet (SMM) behavior with a non-negligible anisotropy barrier (U_{eff}) of 42 K.

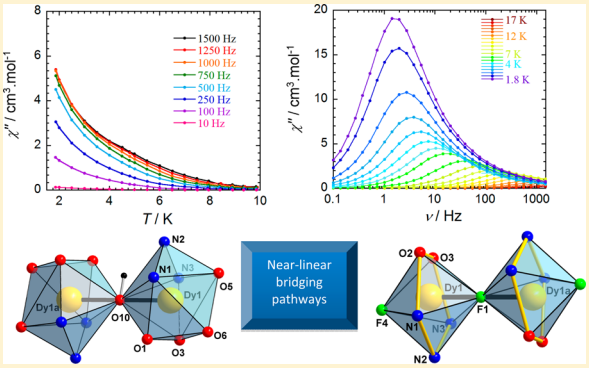

INTRODUCTION

Recent research into nanoscale magnetic materials has led to lanthanide ions becoming prime candidates in the synthesis of coordination complexes. This can be partly attributed to their inherently large spin−orbit coupling, thus leading to significant magnetic anisotropy.[1] Such anisotropy is known to lead to a magnet-like behavior of slow relaxation of the magnetization in these systems. Metal complexes which display these exciting physical properties belong to a class of new magnetic materials, termed single-molecule magnets (SMMs), that can potentially be employed in various high-tech devices such as memory storage and quantum computers.[2] The magnetic orbitals in lanthanide ions are located in the core 4*f* orbitals; thus, superexchange pathways generally play a minimal role in the magnetic interactions.[3] Recent research, however, determined that the large anisotropy and non-negligible magnetic moments of lanthanide ions compensate for the weak exchange coupling and have yielded SMMs with the highest spin reversal barriers to date.[4] Some of our recent studies involving a series of lanthanide complexes containing $\{Dy_2\}$ cores have resulted in high energy barriers for the reversal of the magnetization when coordinated to the Schiff-base H_2valdien ligand.[5] It was also discovered that the nature and strength of the magnetic interaction between metal ions can be strongly influenced by changes in the coordination environment of the metal center. As an example, we have demonstrated that the use of stronger electron withdrawing groups on capping ligands, while maintaining a structurally comparable core, can indeed have a drastic impact on the magnetic relaxation.[5b] Similarly, the bridging ligands, which act as potential superexchange pathways, are also a key component in controlling the resulting magnetic behavior where the nonmagnetic ligands mediate the magnetic coupling between metal ions. In fact, even the weakest coupling between two lanthanide ions can give way to unique magnetic behavior such as intramolecular entanglement.[5c] Investigations on the type of magnetic interactions, or lack thereof, which can be obtained from a specific type of bridging moiety can provide further insight into understanding magnetic behaviors leading toward higher energy barriers. Consequently, we report the synthesis, structure, and magnetic properties of two new lanthanide complexes featuring rare bridging pathways for coordination complexes. The structural element of a single hydroxide- or fluoride-bridge, in a near-linear or linear fashion, between two metal centers proves to be quite uncommon for lanthanide coordination complexes, with only three examples in the literature to date. Two dinuclear Eu^{III}-based systems have been reported by R. Tripier and co-workers containing a linear Eu−F−Eu entity,[6] while the compound by Z. Shi et al. exhibits a 1D zigzag chain with Dy_2 cores bridged by unsupported fluoride anions, resulting in slow relaxation of the magnetization under zero field.[7] Also notable is the work of J. Bendix and co-workers for their magnetic studies carried out on 3*d*−4*f* systems which effectively

Received: February 12, 2015
Published: June 19, 2015

DOI: 10.1021/acs.inorgchem.5b00343
Inorg. Chem. 2015, 54, 6195−6202

Scheme 1. Synthesis of the H_2valdien Ligand

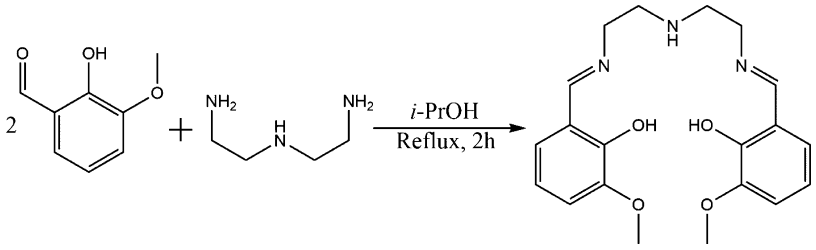

display the potential of unsupported fluoride-bridges for exhibiting slow magnetic relaxation.[8] The high demand for molecular magnetic systems with unsupported fluoride-bridged linkages, due to their relative scarcity, is well-discussed in a recent review by the aforementioned authors.[9] Furthermore, it is interesting to note that a few lanthanide organometallic complexes do contain linear lone oxo-bridges; however, the oxide products were often not intended as the reactions were performed in inert atmosphere.[10] Alternatively, to our knowledge, there is only one example of a magnetic study carried out on pure lanthanide coordination complexes with single near-linear or linear hydroxo- or fluoro-bridges.[7] Therefore, we set out to investigate the resulting magnetic interactions from these unusual bridging pathways for lanthanide coordination complexes. The simplicity of dinuclear cores with centrosymmetry allows for a better understanding of the magnetic interaction between two spin carriers. The static and dynamic susceptibility measurements reveal that both complexes exhibit ferromagnetic coupling between the two Dy^{III} centers as well as slow relaxation of the magnetization.

EXPERIMENTAL SECTION

General Considerations. All manipulations were performed under aerobic/ambient conditions. All materials were used as received from Aldrich, TCI America, and Strem Chemicals without further purification.

Synthesis of N1,N3-Bis(3-methoxysalicylidene)diethylenetriamine (H_2valdien). The H_2valdien ligand was synthesized according to a previously reported method,[5a] with a slight modification (Scheme 1). The change of solvent from EtOH to *i*-PrOH has shown to facilitate the precipitation process.

To a solution of *o*-vanillin (3.80 g, 0.025 mol) in 30 mL of isopropyl alcohol, dried through molecular sieves, was added a solution of diethylenetriamine (1.23 mL, 0.0125 mol) in 10 mL of isopropyl alcohol. The resulting orange solution was refluxed for 2 h, and after cooling to room temperature, the solvent was removed under reduced pressure to give an orange oil. The latter oil was left to stand overnight in a refrigerator at a temperature of 5 °C from which a yellow precipitate was collected by suction filtration and washed with diethyl ether. Yield = 96%. NMR ^{1}H ($CDCl_3$, 400 MHz): δ 2.97 (t, 2H, CH_2—N), 3.69 (t, 2H, CH_2—N), 3.88 (s, 3H, OCH_3), 6.90 (t, 1H, Ar), 6.99 (d, 2H, Ar), 8.32 (s, 1H, N=CH). Selected IR (cm^{-1}): 3419 (w), 3056 (w), 2995 (w), 2935 (w), 2900 (w), 2835 (w), 1629 (m), 1468 (s), 1416 (m), 1376 (w), 1335 (w), 1269 (s), 1146 (w), 1128 (w), 1080 (m), 1024 (w), 964 (m), 875 (m), 838 (m), 778 (m), 734 (s), 665 (w).

*Preparation of $[Na_2Dy^{III}_2(valdien)_2(\mu\text{-}OH)(dbm)_2(H_2O)_2]$-$[Na_2Dy^{III}_2(valdien)_2(\mu\text{-}OH)(dbm)_2(NO_3)_2]$ (**1**).* The reaction of dibenzoylmethane (Hdbm) (0.17 g, 0.75 mmol), H_2valdien (0.090 g, 0.25 mmol), and NaOH (0.060 g, 1.50 mmol) in 8 mL of MeOH and 5 mL of MeCN with $Dy(NO_3)_3{\cdot}6H_2O$ (0.11 g, 0.25 mmol) in 2 mL of MeOH resulted in a clear yellow solution. The resulting filtrate was placed in a diethyl ether bath to assist the crystallization process. After 2 days, X-ray quality colorless rectangular-shaped crystals of **1** were isolated with a yield of 68%. Selected IR (cm^{-1}): 3287 (w), 3152 (w), 2890 (w), 1624 (s), 1596 (s), 1557 (m), 1519 (s), 1470 (s), 1401 (s), 1324 (s), 1215 (s), 1167 (m), 1108 (w), 1077 (m), 1040 (w), 1029 (w), 973 (m), 943 (w), 921 (m), 858 (m), 831 (m), 782 (w), 733 (s), 722 (s), 690 (m), 623 (m), 610 (m). Elemental analysis expected: C 50.60%, H 4.49%, N 5.82%. Found: C 50.53%, H 4.28%, N 5.66%.

*Preparation of $[Na_3Dy^{III}_2(valdien)_2(\mu\text{-}F)(\mu_3\text{-}F)_2(Cl)_2(MeOH)_2]_n{\cdot}0.5(MeOH){\cdot}(H_2O)$ (**2**).* Complex **2** was produced by the reaction of $DyCl_3{\cdot}6H_2O$ (0.094 g, 0.25 mmol) in 5 mL of MeOH with H_2valdien (0.092 g, 0.25 mmol) and Et_3N (70 μL, 0.50 mmol) in 5 mL of MeOH and 5 mL of MeCN. The reagents were refluxed for 1 h at 80 °C. When cooled to room temperature, NaF (0.031 g, 0.75 mmol) was added to the reaction mixture giving a yellow solution. The resulting solution was placed in a diethyl ether bath to facilitate crystallization. Colorless rectangular crystals suitable for X-ray crystallography were obtained over a period of 5 days with a yield of 35%. Selected IR (cm^{-1}): 3568 (w), 3371 (br), 3211 (w), 2901 (w), 2834 (w), 2162 (w), 1979 (w), 1629 (s), 1598 (m), 1552 (w), 1470 (s), 1454 (s), 1406 (m), 1320 (m), 1233 (m), 1216 (s), 1169 (w), 1110 (m), 1079 (m), 1042 (w), 1044 (w), 973 (m), 933 (w), 914 (w), 857 (m), 834 (w), 784 (w), 726 (s), 623 (m). Elemental analysis expected: C 37.57%, H 4.30%, N 6.19%; %, F 4.19%. Found: C 37.76%, H 4.11%, N 6.44%, F 4.02%.

*Preparation of $[Na_2Gd^{III}_2(valdien)_2(\mu\text{-}OH)(dbm)_2(H_2O)_2]$-$[Na_2Gd^{III}_2(valdien)_2(\mu\text{-}OH)(dbm)_2(NO_3)_2]$ (**3**).* Compound **3** was prepared following the same procedure as complex **1**, using $Gd(NO_3)_3{\cdot}6H_2O$ (0.11 g, 0.25 mmol). X-ray quality colorless rectangular crystals were recovered after 2 days. Yield: 66%. Selected IR data (cm^{-1}): 3281 (w), 2888 (w), 1623 (m), 1596 (m), 1518 (m), 1470 (s), 1452 (s), 1400 (s), 1324 (s), 1233 (m), 1214 (s), 1167 (w), 1108 (w), 1077 (m), 1039 (w), 972 (m), 942 (w), 917 (m), 857 (m), 828 (m), 733 (s), 722 (s), 691 (m), 622 (m), 610 (m). Elemental analysis expected: C 51.04%, H 4.38%, N 5.95%. Found: C 50.78%, H 4.21%, N 5.90%.

Physical Measurements. X-ray crystallographic data were collected on single colorless crystals mounted on a glass fiber for complexes **1**–**3**. Unit cell measurements and intensity data collections were performed on a Bruker-AXS SMART 1 k CCD diffractometer using graphite monochromated Mo Kα radiation (λ = 0.710 73 Å). The data reduction included a correction for Lorentz and polarization effect, with an applied multiscan absorption correction (SADABS).[11] The crystal structures were solved and refined using the SHELXTL program suite.[12] Direct methods yielded all non-hydrogen atoms which were refined with anisotropic thermal parameters. All hydrogen atom positions were calculated geometrically and were riding on their respective atoms. Crystallographic data for the structures reported in this paper have been deposited with the Cambridge Crystallographic Center as supplementary publication no. CCDC 990947–990949. Crystallographic data is presented in Table S1 of the Supporting Information.

Infrared spectroscopy was performed on a Nicolet 6700 FT-IR spectrometer in the 400–4000 cm^{-1} range.

NMR analyses were conducted using the Bruker Avance 400 MHz spectrometer equipped with an automatic sample charger and a 5 mm autotuning broadband probe with Z gradient.

The magnetic susceptibility measurements were obtained using a Quantum Design Superconducting Quantum Interference Device (SQUID) magnetometer MPMS-XL7 that works between 1.8 and 300 K for direct current (dc) applied fields ranging from −7 to 7 T.

DOI: 10.1021/acs.inorgchem.5b00343
Inorg. Chem. 2015, 54, 6195–6202

Measurements were performed on restrained crushed polycrystalline samples of 14.2, 18.8, and 15.0 mg of complexes **1**−**3**, respectively, wrapped in a polyethylene membrane. Alternating current (ac) susceptibility measurements were performed under an oscillating ac field of 3 Oe and ac frequencies that ranged from 0.1 to 1500 Hz. The magnetization data was collected at 100 K to check for ferromagnetic impurities that were absent in all samples. All magnetic data were corrected for the sample holder as well as other diamagnetic contributions.

Elemental analysis was performed at the Université de Montréal.

RESULTS AND DISCUSSION

Syntheses. The H_2valdien ligand has been synthesized following a known procedure with slight modifications:[5a] a Schiff-base reaction between the primary amine groups of diethylenetriamine and the aldehyde group of *o*-vanillin. The increasingly well-known H_2valdien ligand is an ideal candidate to encapsulate the larger lanthanide ions due to its flexibility as well as presenting two possible coordination pockets which can encapsulate the metal center.[5,13] The presence of multiple coordination pockets, such as the N_3O_2 and O_4 donor sets of H_2valdien, encourages the formation of multinuclear 4*f* complexes while also allowing a certain degree of control over the interaction between metal centers. In the cases of **1** and **2**, the Dy^{III} ions occupy the N_3O_2 pocket while the sodium cations take up the O_4 donor sets (Figure 1). The coordination of the H_2valdien ligands to the metal ions is promoted by the full deprotonation of the molecules through the addition of a base, such as Et_3N or NaOH, which enables the phenoxides to act as bridging groups in both coordination pockets. Complex **1** also incorporates an additional chelating ligand, the dbm^- (dibenzoylmethanido) anion, which can exist in two possible tautomeric forms. Under the basic conditions of the synthesis, the negatively charged enol form of dbm^- is favored. These dbm^- molecules serve as capping agents forming six-membered coordination rings with the Dy atoms resulting in isolated molecular entities. For compound **2**, the addition of NaF was initially used to introduce fluoride anions as secondary ligands; however, single-crystal X-ray crystallography revealed that the sodium cations had linked the $\{Dy_2\}$ units forming a stable one-dimensional coordination polymer.

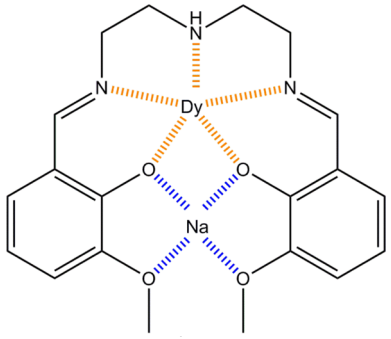

Figure 1. Coordination pockets of the valdien^{2-} ligand observed in **1** and **2**. Color code: orange bonds (N_3O_2 pocket) and blue bonds (O_4 pocket).

Structural Analysis. The molecular structures of **1** and **2**, obtained through single-crystal X-ray data are shown in Figures 2 and 3, respectively. The structural analysis of compound **1**

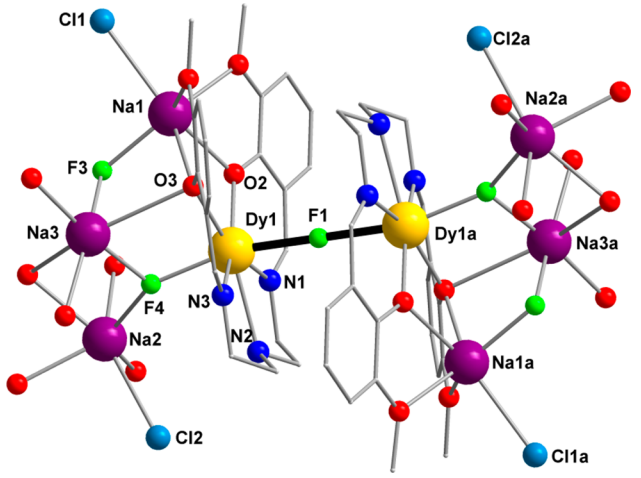

Figure 3. Molecular structure of the dinuclear unit in compound **2**. Selected symmetry equivalent atoms are denoted by an additional "a" in the label. The lone linear fluoro-bridge is shown in black bonds. Color code: green (F), yellow (Dy^{III}), red (O), blue (N), purple (Na), light blue (Cl), and gray (C). Hydrogen atoms and solvent of crystallization have been omitted for clarity.

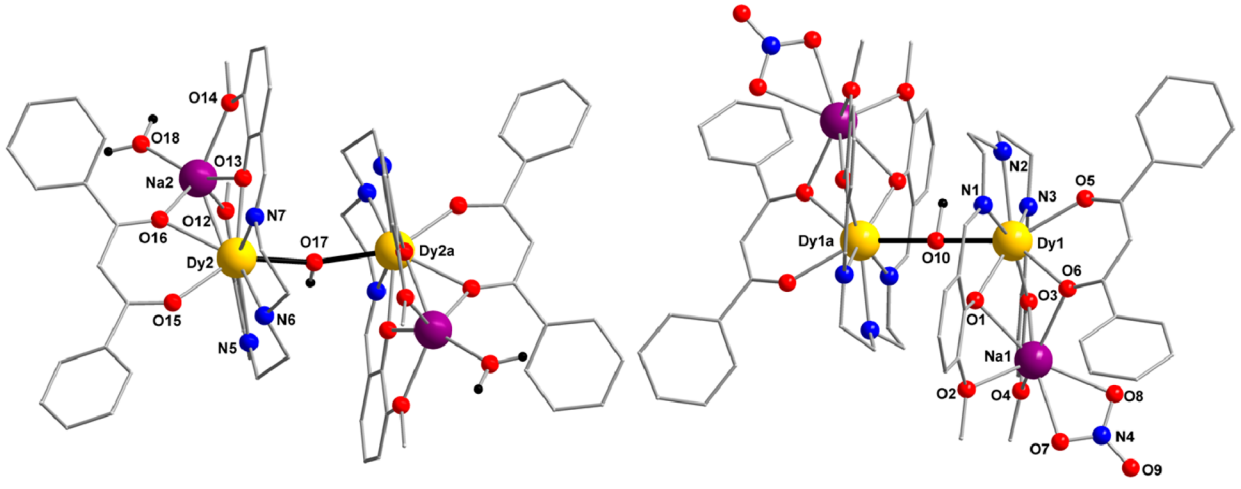

Figure 2. Molecular structures of compound **1A** (left) and **1B** (right). Symmetry equivalent labels are denoted by an additional "a" in the label (Dy1a and Dy2a). The lone hydroxo-bridges are shown in black bonds. Color code: yellow (Dy^{III}), red (O), blue (N), purple (Na), gray (C), black (H). Selected hydrogen atoms are omitted for clarity.

DOI: 10.1021/acs.inorgchem.5b00343
Inorg. Chem. 2015, 54, 6195−6202

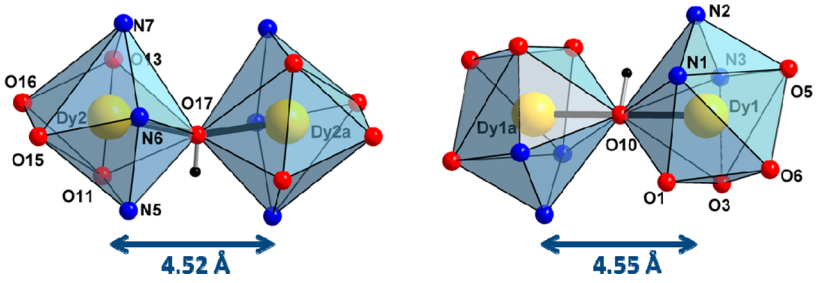

Figure 4. Coordination polyhedra of the Dy^{III} ions showing the distorted dodecahedral geometry in **1A** (left) and **1B** (right).

shows a dinuclear core in which the Dy^{III} atoms are eight-coordinate and adopt a distorted dodecahedral geometry (Figure 4). In comparison, compound **2** presents a polymeric chain of $\{Dy_2\}$ units, where the metal centers are seven-coordinate and are in a distorted pentagonal bipyramidal geometry (Figure 5). Complex **1** crystallizes in the monoclinic

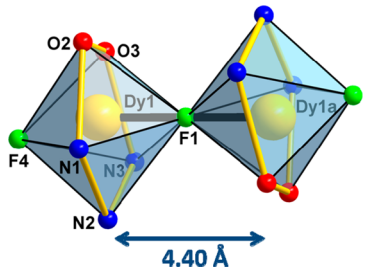

Figure 5. Coordination polyhedron of the Dy^{III} ions showing the slightly distorted pentagonal bipyramid in **2**.

$P2_1/n$ space group and exhibits centrosymmetric geometry where the central oxygen atoms (O10 and O17) lie on an inversion center. The element of centrosymmetry is strongly supported by the fact that refinement in a different space group resulted in a visible increase of the final R_f values. On the other hand, compound **2** crystallizes in the triclinic $P\bar{1}$ space group forming a chain consisting of a repeating unit of four Dy^{III} ions through the connection of two $\{Dy_2\}$ dimers. Each of the $\{Dy_2\}$ cores displays centrosymmetric geometry through the inversion centers which lie on F1 and F2. In both complexes, the potential magnetic superexchange pathway between Dy^{III} ions is composed of a single bridging group, a hydroxide for **1** and a fluoride ion for **2**. It is important to note that, in the case of **2**, the assignment of the central atom is not trivial due to the isoelectronic nature of fluoride and hydroxide anions. The higher stability of the fluoride anion, due to electronegativity effects, as well as the striking similarities between the Dy^{III}–F distances for **2** (2.20 and 2.21 Å for Dy1–F1 and Dy2–F2, respectively) and the only other reported single fluoride-bridge between two Dy^{III} ions (2.22 Å), strongly suggests the assignment of fluoride;[7] however, the nature of the bridging ligand cannot be unambiguously determined. The coordination spheres of all Dy^{III} metal centers in **1** and **2** both include three nitrogen atoms and two oxygen atoms belonging to the pentadentate valdien^{2-} ligand and therefore take up the N_3O_2 coordination pocket. It is noteworthy that the single-crystal X-ray crystallography study for **1** revealed two dinuclear complex in the same unit cell. The $[Na_2Dy^{III}_2(valdien)_2(\mu\text{-OH})(dbm)_2(H_2O)_2]^+$ cation will hereafter be referred to as **1A**, while the $[Na_2Dy^{III}_2(valdien)_2(\mu\text{-OH})(dbm)_2(NO_3)_2]^-$ anion will be **1B**. In complex **1**, the coordination sphere is completed by an additional two oxygen atoms (O15 and O16 for **1A** and O5 and O6 for **1B**) from dbm$^-$ and another oxygen atom originating from a hydroxide ion (O17 in **1A** and O10 in **1B**), while in **2**, two fluorides take up the axial positions of the pentagonal bipyramid. For **2**, the Dy1–F1–Dy1a and Dy2–F2–Dy2a angles have been determined to be ~180°. In both compounds, Na^+ ions occupy the O_4 coordination pocket of the valdien^{2-} ligand. In complex **1**, the distance separating Dy1–Dy1a and Dy2–Dy2a is 4.55 and 4.52 Å, respectively, longer than typical Dy^{III} dimers bridged by two hydroxides,[14] while **2** has a separation of 4.40 and 4.42 Å between Dy1–Dy1a and Dy2–Dy2a, respectively. Selected bond distances and angles for **1** and **2** are presented in Table 1.

Table 1. Selected Bond Distances (Å) and Angles (deg) for 1 and 2

Compound **1**			
Dy1–N1	2.515(3)	Dy2–N5	2.549(4)
Dy1–N2	2.545(3)	Dy2–N6	2.554(3)
Dy1–N3	2.563(3)	Dy2–N7	2.569(4)
Dy1–O1	2.294(2)	Dy2–O11	2.268(3)
Dy1–O3	2.253(2)	Dy2–O13	2.270(3)
Dy1–O5	2.405(2)	Dy2–O15	2.362(2)
Dy1–O6	2.447(3)	Dy2–O16	2.451(3)
Dy1–O10	2.272(1)	Dy2–O17	2.299(8)
O5–Dy1–O6	69.26(8)	O15–Dy2–O16	68.39(9)
Dy1–O10–Dy1a	180.00	Dy2–O17–Dy2a	160.48
Compound **2**			
Dy1–F1	2.202(3)	Dy2–F2	2.209(2)
Dy1–F4	2.137(4)	Dy2–F3	2.141(4)
Dy1–N1	2.518(6)	Dy2–N4	2.502(6)
Dy1–N2	2.505(6)	Dy2–N5	2.509(6)
Dy1–N3	2.530(6)	Dy2–N6	2.516(6)
Dy1–O2	2.239(4)	Dy2–O6	2.238(4)
Dy1–O3	2.278(5)	Dy2–O7	2.273(5)
Dy1–Dy1a	4.403(4)	Dy2–Dy2a	4.418(4)
Dy1a-Dy2	5.050(4)	Dy1–F1–Dy1a	180.00
Dy2–F2–Dy2a	180.00		

Furthermore, in both compounds the valdien^{2-} ligand molecules form a plane which is perpendicular to the lone bridge. In compound **1**, however, the dbm$^-$ groups are positioned toward the extremities of the molecule and form bite angles of 69.26° and 68.39° for Dy1 and Dy2, respectively. These dbm$^-$ molecules act as capping agents and lead to the formation of well-isolated compounds (Figure 2), whereas in **2**, the Na^+ ions play a key role in the formation of a stable one-dimensional coordination polymer (Figure 3). The repeating unit of the chain is shown in Figure S1 in the Supporting Information.

DOI: 10.1021/acs.inorgchem.5b00343
Inorg. Chem. 2015, 54, 6195–6202

In molecule **1A**, terminal H_2O groups are coordinated to Na2 (Figure 2, left), while in **1B**, terminal NO_3^- are coordinated to the corresponding Na1 ions (Figure 2, right). Due to the different bridging modes observed between nitrate, which is bidentate, and the water molecules, which are monodentate, the resulting geometry of the Na^+ ions is affected. More precisely, in the structure of **1A**, the Na2 ions adopt a trigonal prismatic geometry whereas, in **1B**, the Na1 ions are in a square face monocapped trigonal prism arrangement. An additional difference in the molecular structures of **1A** and **1B** to consider is the bridging of the μ-OH groups. Compound **1B** would represent the first example, to our knowledge, of a linear hydroxo-bridge forming a Dy1−O10−Dy1a angle as close as possible to 180°. However, in the case of **1A**, there is a 50%−50% disorder on the μ-OH oxygen atom forming a Dy2−O17−Dy2a angle of 160.5°. This variation of the bridging angle in the μ-OH moiety may be caused by the structural differences between the two molecules, which were previously mentioned. With the purpose of verifying that the central oxygen atoms (O10 and O17) are in fact hydroxo-bridges, bond valence sum (BVS) calculations were carried out on these O atoms. The BVS values for both corresponded to 1, indicating that the oxygen atoms are monoprotonated (Supporting Information, Table S2). In order to ascertain the accuracy of our calculations, we applied the same equation on compounds consisting of two Dy^{III} ions bridged by an oxo center, as well as a Dy_4 aggregate bridged by a μ_4-OH moiety, where in both cases the calculations correctly predicted BVS values of 2 and 1, respectively, for the oxygen atoms.[10f,15]

The packing diagram for **1** along the *a* axis, presented in Figure 6, shows discrete dinuclear units with a zig-zag arrangement of the molecules. This can also be illustrated along the *b* and *c* axes from Supporting Information Figures S2 and S3, respectively. We can also observe an antiparallel arrangement between the layers with the closest metal−metal distance of 10.14 Å between the neighboring units. Close inspection also reveals the presence of hydrogen bonding between O18 of the terminal water molecule and O8 of an adjacent nitrate group, which occurs through a distance of 2.77 Å. For **2**, it can be seen from the packing arrangement along the *b* axis in Figure 7 that the dinuclear units are linked via Na^+ ions into chains (this can also be seen in the packing diagrams along the *a* and *c* axes in the Supporting Information, Figures S4 and S5, respectively). The chains are arranged in a parallel fashion with the closest interchain metal−metal distance of 11.80 Å.

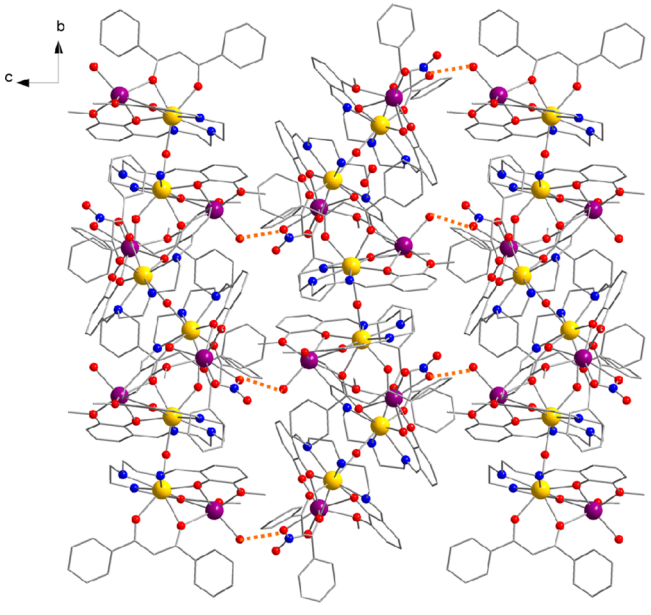

Figure 6. Packing arrangement of **1** along the *a* axis showing the antiparallel ordering of the molecules, as well as the intermolecular hydrogen bonding as shown by the orange dotted lines. Color code: yellow (Dy), red (O), blue (N), purple (Na), and gray (C).

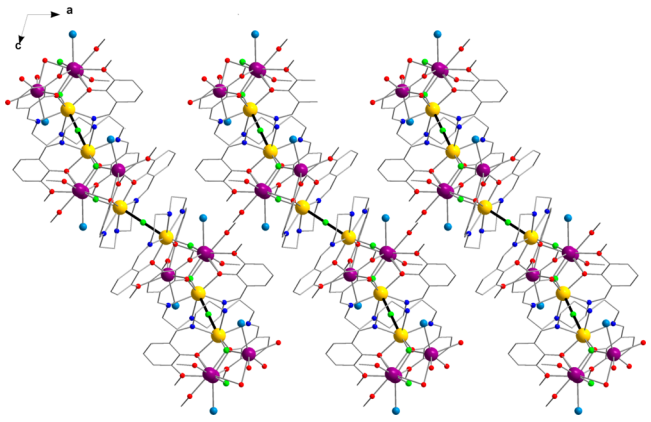

Figure 7. Packing arrangement of **2** along the *b* axis showing chains aligned in a parallel fashion highlighting the lone linear bridges in black. Color code: yellow (Dy), red (O), blue (N), light blue (Cl), purple (Na), green (F), and gray (C). Methanol and water solvent molecules are omitted for clarity.

The structural element of a near-linear lone hydroxo-bridge proves to be a rare feature among metal complexes, where only a handful have been reported to date.[16] It is worth mentioning that **1A** and **1B** are the first lanthanide-only compounds containing this structural element. A few examples exist in the literature for transition metal compounds containing single hydroxo-bridges unsupported by ancillary ligands, notably a dinuclear iron(III) compound with a Fe−O−Fe angle of 173.60° by C. A. Reed et al.,[16b] as well as another dinuclear iron(III) compound synthesized by C. A. Grapperhaus and co-workers giving a corresponding Fe−O−Fe angle of 166.70°.[16d] It is interesting to point out that both compounds are cationic species as in the case of **1A**. In similar fashion to the hydroxo-bridge, a linear or near-linear lone fluoro-bridge proves to be just as uncommon, where, to our knowledge, there exists only three reported pure lanthanide coordination compounds exhibiting this feature.[6,7] Consequently, we set out to investigate the type of magnetic interaction that would arise from such unique bridging pathways.

Magnetic Properties. It must be noted that while the metal centers in both compounds are encapsulated in similar fashion by the valdien^{2-} ligand as well as display a similar type of bridging, their inherent structural differences (i.e., seven vs eight coordination numbers) will have a significant impact on both the dc and ac magnetic susceptibilities due to the change in crystal field splitting. Therefore, the following analysis of the magnetic behaviors of **1** and **2** is of two very distinct systems. The dc magnetic susceptibility measurements for both **1** and **2** were performed between 1.8 and 300 K under an applied dc field of 1000 Oe. The χT versus T plots of **1** and **2** are presented in Figure 8, where the χT product at room

DOI: 10.1021/acs.inorgchem.5b00343
Inorg. Chem. 2015, 54, 6195−6202

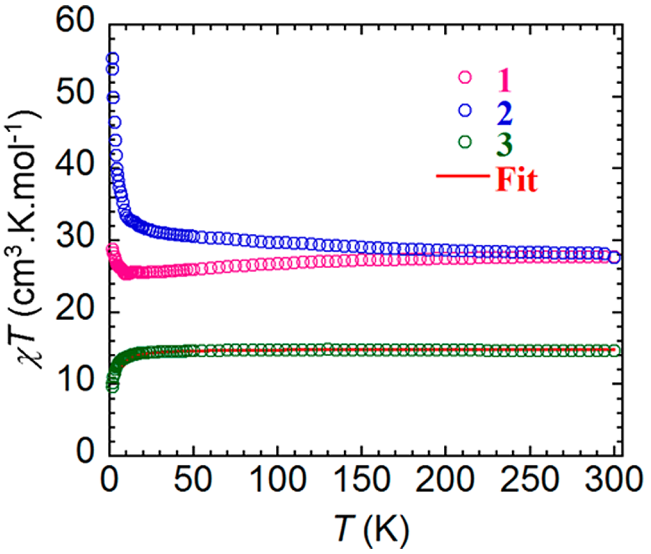

Figure 8. Temperature dependence of the χT product at 1000 Oe for compounds **1** (pink), **2** (blue), and **3** (green) with χ being the molar magnetic susceptibility equal to M/H per mole of the compound. The solid line corresponds to the best fit for **3**.

temperature is 27.74 cm^3 K mol^{-1} for **1** and 27.62 cm^3 K mol^{-1} for **2**, which is within reasonable agreement of the expected value of 28.34 cm^3 K mol^{-1} for two uncoupled Dy^{III} ions ($^6H_{15/2}$, $S = {}^5/_2$, $L = 5$, $g = {}^4/_3$). For **1**, the χT values remain relatively constant before reaching a minimum value of 25.3 cm^3 K mol^{-1} at 11 K and then increasing sharply to a maximum value of 28.76 cm^3 K mol^{-1} at 2 K. In compound **2**, the χT product continuously increases reaching a maximum of 55.4 cm^3 K mol^{-1} at 1.8 K. For both compounds, the increase of χT at low temperatures is indicative of intramolecular ferromagnetic coupling between the metal centers. This weak interaction is negligible at high temperature and is often masked at high temperatures by the thermal population of the excited states of Dy^{III} ions, as is commonly observed in lanthanide compounds.[17] In order to probe the strength of the magnetic interaction between lanthanide ions, the synthesis of Gd^{III} analogues is common practice due to its isotropic nature.[18] While we successfully synthesized the Gd^{III} analogue of **1**, identified as compound **3**, we were unsuccessful in obtaining an identical analogue of **2**. At room temperature, the χT product of **3** was determined to be 14.60 cm^3 K mol^{-1}, which is in good agreement with the expected value of 15.76 cm^3 K mol^{-1} for two uncoupled Gd^{III} ions ($^8S_{7/2}$, $S = {}^7/_2$; $L = 0$, $g = 2$). Furthermore, it can be seen from Figure 8 that the magnetic interaction between metal ions changes from ferromagnetic for Dy^{III}, to antiferromagnetic in Gd^{III}, revealed by the decrease of the χT value when lowering the temperature. A few examples of this behavior have been previously reported and are explained by the variation of the effective magnetic dipole moment at low temperatures due to f–f interactions.[19] The application of the van Vleck equation to Kambe's vector coupling scheme by using the isotropic spin Hamiltonian $H = -2JS_a \cdot S_b$ with $S_a = S_b = {}^7/_2$ allows us to reproduce the variation of χT versus T. The best-fit parameters obtained are $J = -0.051(3)$ cm^{-1} and $g = 1.93(9)$. The exchange interaction for a pure lanthanide dinuclear system through a single hydroxo-bridge is therefore quite weak, due to the shielded f orbitals which prevent adequate overlap with bridging ligand orbitals. It is interesting to note, however, that while unsuccessful in obtaining the Gd^{III} analogue of **2**, it can be seen from the χT versus T plot that the increase of the χT product at low temperature is more pronounced in **2** at temperatures below 20 K. This behavior may suggest a stronger interaction between metal centers bridged by a single fluoride ion rather than a single hydroxide-bridge; however, the difference in the χT product could also be attributed to a change in the eigenvectors of the ground state.

Field dependence of the magnetization, M, measurements show a rapid increase in the magnetization at low fields up to 10.1 μ_B (**1**) and 10.5 μ_B (**2**) at 1.8 K and 7 T (Figure 9).

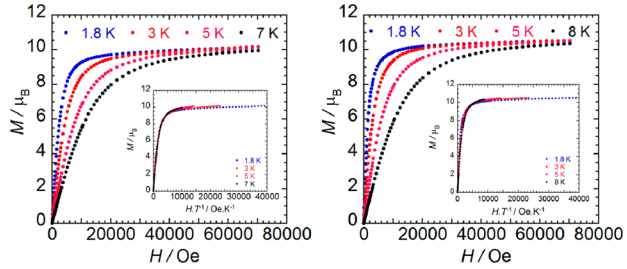

Figure 9. Field dependence of the magnetization, M, at the indicated temperatures for compounds **1** (left) and **2** (right) illustrating the nonsaturation. Inset: M versus HT^{-1} plot showing nonsuperposition of the magnetization curves at different temperatures.

Additionally, the M versus HT^{-1} plots (Figure 9, insets), at varying temperatures, show magnetization curves that are not surperimposable on a single master curve. Consequently, these plots suggest the presence of non-negligible magnetoanisotropy and/or low-lying excited states for compounds **1** and **2**. In the case of the Gd^{III} analogue, the observed saturation of 12.91 μ_B at 7 T (Supporting Information Figure S6) is within reach of the theoretical value of 14.00 μ_B ($g = 2.00$) for two Gd^{III} ions. Moreover, the magnetization curve can be fit using a Brillouin function, which allows for a comparison of the g value derived from the χT versus T fit. Using this method, a g value of 1.87 was obtained, which is comparable to the value calculated through the χT versus T fit mentioned previously.

Alternating current (ac) magnetic measurements were performed on **1** and **2** under zero dc field, in order to investigate potential slow relaxation of the magnetization originating from SMM behavior. For **1**, the in-phase, χ', plot shows a frequency-dependent signal under zero applied dc field (Figure 10, left). We can also observe a slight shoulder structure around 5.5 K which can be more visible in the out-of-phase component χ''. This shoulder in both the real (χ') and imaginary (χ'') components of the ac magnetic susceptibility measurements indicates the presence of multiple relaxation processes that can in part be attributed to the cocrystallization

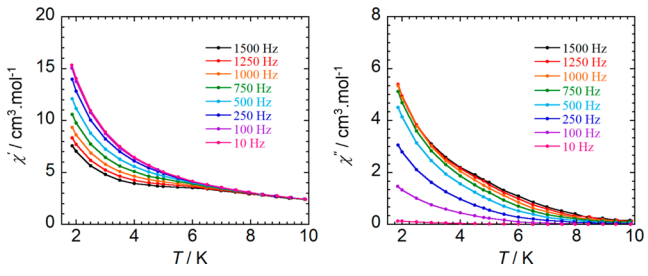

Figure 10. Temperature dependence of the in-phase χ' (left) and out-of-phase χ'' (right) ac susceptibility signals under zero dc field for **1**.

DOI: 10.1021/acs.inorgchem.5b00343
Inorg. Chem. 2015, 54, 6195–6202

of the two structurally different $\{Dy_2\}$ units. Furthermore, a frequency-dependent tail of a peak can be observed in the variation of χ'', for measurements that lie at temperatures below 1.8 K (Figure 10, right), the operating limit of our SQUID. Such χ'' signals are indicative of a slow magnetization relaxation process and suggest possible SMM behavior.[20] The presence of merely tails of peaks rather than full peaks reveals that the slow relaxation of the magnetization is highly influenced by the quantum tunneling of the magnetization (QTM) through the spin reversal barrier commonly found in dinuclear lanthanide SMMs.[21] Furthermore, without a clearly defined peak it is difficult to quantify the energy barrier that prevents the reversal of the spins. One method to shortcut the QTM involves the application of a dc field during the ac measurements. With the application of a 1000 Oe dc field on a polycrystalline sample of **1**, the emergence of frequency-dependent ac peaks could be clearly observed in the out-of-phase measurements (Figure S7 of the Supporting Information). This confirms the presence of significant QTM, and thus, compound **1** can be considered as a field-induced SMM.

For compound **2**, ac measurements performed with zero dc field resulted in a temperature and frequency-dependent signal below 17 K. The χ'' component of the ac susceptibility clearly exhibits a frequency-dependent full peak with one maximum (Figure 11). This is indicative of superparamagnet-like behavior

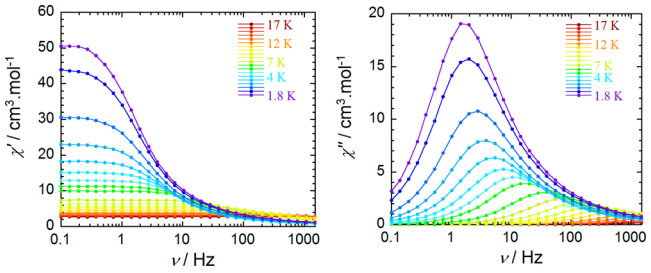

Figure 11. Frequency dependence of the in-phase χ' (left) and out-of-phase χ'' (right) ac susceptibility signals under zero dc field for **2**.

of slow magnetization relaxation of a SMM. The thermally activated relaxation follows an Arrhenius-like behavior ($\tau = \tau_0 \exp(U_{eff}/kT)$), where the anisotropy energy barrier obtained from the fitting is $U_{eff} = 42$ K ($\tau_0 = 5.54 \times 10^{-6}$ s) (Figure S8 of the Supporting Information).

In order to further investigate the relaxation mechanism of **2**, the graphical representation of χ'' versus χ' (Cole−Cole plot) in the temperature range 1.8−14 K confirms the presence of a single relaxation process (Figure 12). At temperatures below 2 K, QTM causes a slight distortion of the semicircles, while at

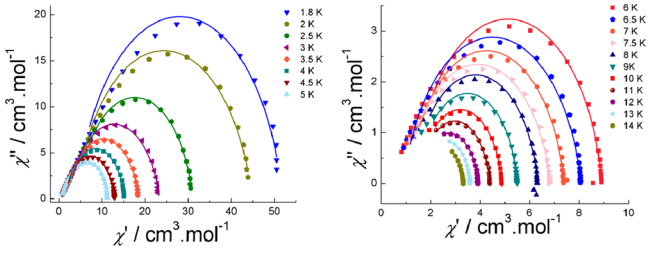

Figure 12. Cole−Cole plots for **2** in the temperature range 1.8−5 K (left) and 6−14 K (right) using the ac susceptibility data. The solid lines correspond to the best fit obtained with a generalized Debye model.

higher temperatures, more symmetrical semicircles can be obtained. The data can be fitted using a generalized Debye model. The α values range from 0.03 up to 0.19 where the α parameter has a tendency to be inversely proportional to the temperature. In other words, with decreasing temperatures we can expect an increase of the α values. This is in part due to the QTM which occurs at low temperatures.

CONCLUSION

The use of H_2valdien, an encapsulating Schiff-base ligand, coupled with ancillary ligands, has allowed the synthesis of three centrosymmetric lanthanide dimers which were fully characterized. These compounds exhibit unique bridging pathways for lanthanide coordination complexes. The lone hydroxo-bridge, which effectively separates the Dy^{III} ions in the discrete molecules of **1**, and similarly, the fluoride moieties of the coordination polymer of **2**, both induce ferromagnetic interactions between metal centers. However, the Gd^{III} analogue of **1** revealed weak intramolecular antiferromagnetic interactions giving a $J = -0.05$ cm^{-1}. Furthermore, the Dy^{III} analogue of **1** exhibits slow relaxation of the magnetization, as demonstrated under an applied field, while **2** displays SMM behavior at zero-field with an anisotropic barrier of $U_{eff} = 42$ K. To achieve our goal of isolating compounds with increasingly higher energy barriers, an understanding of the magnetic behaviors resulting from specific types of bridging pathways will be essential. To this end, the present work reports three new compounds containing rare near-linear unsupported hydroxide- and fluoride-bridges as potential superexchange pathways in lanthanide coordination compounds resulting in slow relaxation of the magnetization.

ASSOCIATED CONTENT

Supporting Information

Crystallographic data (including CIF files), additional structural comparisons, and magnetic measurement plots for **1**−**3**. The Supporting Information is available free of charge on the ACS Publications website at DOI: 10.1021/acs.inorgchem.5b00343.

AUTHOR INFORMATION

Corresponding Author

*E-mail: m.murugesu@uottawa.ca. Phone: 613-562-5800 ext. 2733. Fax: 613-562-5170.

Author Contributions

The manuscript was written through contributions of all authors. All authors have given the approval to the final version of the manuscript.

Notes

The authors declare no competing financial interest.

ACKNOWLEDGMENTS

We thank the University of Ottawa, NSERC, and CIHR (Discovery and RTI grants, Vanier Graduate Scholarship) as well as CFI for their financial support.

REFERENCES

(1) (a) AlDamen, M. A.; Clemente-Juan, J. M.; Coronado, E.; Martí-Gastaldo, C.; Gaita-Ariño, A. *J. Am. Chem. Soc.* **2008**, *130*, 8874−8875. (b) Sessoli, R.; Powell, A. K. *Coord. Chem. Rev.* **2009**, *253*, 2328−2341. (c) Lin, P.-H.; Burchell, T. J.; Ungur, L.; Chibotaru, L. F.; Wernsdorfer, W.; Murugesu, M. *Angew. Chem., Int. Ed.* **2009**, *48*,

DOI: 10.1021/acs.inorgchem.5b00343
Inorg. Chem. 2015, 54, 6195−6202

9489−9492. (d) Woodruff, D. N.; Winpenny, R. E. P.; Layfield, R. A. *Chem. Rev.* **2013**, *113*, 5110−5148.
(2) (a) Bogani, L.; Wernsdorfer, W. *Nat. Mater.* **2008**, *7*, 179−186. (b) Coronado, E.; Day, P. *Chem. Rev.* **2004**, *104*, 5419−5448.
(3) (a) Guo, Y.-N.; Xu, G.-F.; Gamez, P.; Zhao, L.; Lin, S.-Y.; Deng, R.; Tang, J.; Zhang, H.-J. *J. Am. Chem. Soc.* **2010**, *132*, 8538−8539. (b) Rinehart, J. D.; Fang, M.; Evans, W. J.; Long, J. R. *J. Am. Chem. Soc.* **2011**, *133*, 14236−14239. (c) Singh-Wilmot, M. A.; Sinclair, R. A.; Andrews, M.; Rowland, C.; Cahill, C. L.; Murugesu, M. *Polyhedron* **2013**, *53*, 187−192.
(4) (a) Sorace, L.; Benelli, C.; Gatteschi, D. *Chem. Soc. Rev.* **2011**, *40*, 3092−3104. (b) Le Roy, J. J.; Ungur, L.; Korobkov, I.; Chibotaru, L. F.; Murugesu, M. *J. Am. Chem. Soc.* **2014**, *136*, 8003−8010. (c) Guo, P.-H.; Liu, J.-L.; Zhang, Z.-M.; Ungur, L.; Chibotaru, L. F.; Leng, J.-D.; Guo, F.-S.; Tong, M.-L. *Inorg. Chem.* **2012**, *51*, 1233−1235.
(5) (a) Long, J.; Habib, F.; Lin, P.-H.; Korobkov, I.; Enright, G.; Ungur, L.; Wernsdorfer, W.; Chibotaru, L. F.; Murugesu, M. *J. Am. Chem. Soc.* **2011**, *133*, 5319−5328. (b) Habib, F.; Brunet, G.; Vieru, V.; Korobkov, I.; Chibotaru, L. F.; Murugesu, M. *J. Am. Chem. Soc.* **2013**, *135*, 13242−13245. (c) Habib, F.; Lin, P.-H.; Long, J.; Korobkov, I.; Wernsdorfer, W.; Murugesu, M. *J. Am. Chem. Soc.* **2011**, *133*, 8830−8833.
(6) (a) Lima, L. M. P.; Lecointre, A.; Morfin, J.-F.; Blas, D. A.; Visvikis, D.; Charbonnière, L. J.; Platas-Iglesias, C.; Tripier, R. *Inorg. Chem.* **2011**, *50*, 12508−12521. (b) Liu, T.; Nonat, A.; Beyler, M.; Regueiro-Figueroa, M.; Nono, K. N.; Jeannin, O.; Camerel, F.; Debaene, F.; Cianférani-Sanglier, S.; Tripier, R.; Platas-Iglesias, C.; Charbonnière, L. J. *Angew. Chem., Int. Ed.* **2014**, *53*, 7259−7263.
(7) Zhou, Q.; Yang, F.; Liu, D.; Peng, Y.; Li, G.; Shi, Z.; Feng, S. *Inorg. Chem.* **2012**, *51*, 7529−7536.
(8) (a) Dreiser, J.; Pedersen, K. S.; Piamonteze, C.; Rusponi, S.; Salman, Z.; Ali, Md. E.; Schau-Magnussen, M.; Thuesen, C. Aa.; Piligkos, S.; Weihe, H.; Mutka, H.; Waldmann, O.; Oppeneer, P.; Bendix, J.; Nolting, F.; Brune, H. *Chem. Sci.* **2012**, *3*, 1024−1032. (b) Thuesen, C. Aa.; Pedersen, K. S.; Schau-Magnussen, M.; Evangelisti, M.; Vibenholt, J.; Piligkos, S.; Weihe, H.; Bendix, J. *Dalton Trans.* **2012**, *41*, 11284−11292.
(9) Pedersen, K. S.; Sørensen, M. A.; Bendix, J. *Coord. Chem. Rev.* **2015**, *299*, 1−21.
(10) (a) Adam, M.; Massarweh, G.; Fischer, R. D. *J. Organomet. Chem.* **1991**, *405*, C33−C37. (b) Evans, W. J.; Grate, J. W.; Bloom, I.; Hunter, W. E.; Atwood, J. L. *J. Am. Chem. Soc.* **1985**, *107*, 405−409. (c) Evans, W. J.; Gummersheimer, T. S.; Ziller, J. W. *Appl. Organometal. Chem.* **1995**, *9*, 437−447. (d) Evans, W. J.; Davis, B. L.; Nyce, G. W.; Perotti, J. M.; Ziller, J. W. *J. Organomet. Chem.* **2003**, *677*, 89−95. (e) Zhang, C.; Liu, R.; Zhang, J.; Chen, Z.; Zhou, X. *Inorg. Chem.* **2006**, *45*, 5867−5877. (f) Evans, W. J.; Rego, D. B.; Ziller, J. W. *Inorg. Chem.* **2006**, *45*, 10790−10798. (g) Wooles, A. J.; Cooper, O. J.; McMaster, J.; Lewis, W.; Blake, A. J.; Liddle, S. T. *Organometallics* **2010**, *29*, 2315−2321. (h) Brady, E. D.; Clark, D. L.; Keogh, D. W.; Scott, B. L.; Watkin, J. G. *J. Am. Chem. Soc.* **2002**, *124*, 7007−7015.
(11) *SADABS, Bruker Area Detector Absorption Corrections*; Bruker Analytical X-ray Systems Inc.: Madison, WI.
(12) (a) *SHELXTL, v. 6.12*; Bruker Analytical X-ray Systems Inc.: Madison, WI, 2001. (b) Sheldrick, G. M. *Acta Crystallogr.* **2008**, *A64*, 112−122.
(13) (a) Dou, W.; Yao, J.-N.; Liu, W.-S.; Wang, Y.-W.; Zheng, J.-R.; Wang, D.-Q. *Inorg. Chem. Commun.* **2007**, *10*, 105−108. (b) Parr, J.; Ross, A. T.; Slawin, A. M. Z. *Polyhedron* **1997**, *16*, 2765−2770.
(14) (a) Guo, P.-H.; Meng, Y.; Chen, Y.-C.; Li, Q.-W.; Wang, B.-Y.; Leng, J.-D.; Bao, D.-H.; Jia, J.-H.; Tong, M.-L. *J. Mater. Chem. C* **2014**, *2*, 8858−8864. (b) Chen, R.; Tang, W.; Liang, J.; Jiang, W.; Zhang, Y.; Jia, D. *Dalton Trans.* **2012**, *41*, 12439−12445.
(15) Xue, S.; Zhao, L.; Guo, Y.-N.; Chen, X.-H.; Tang, J. *Chem. Commun.* **2012**, *48*, 7031−7033.
(16) (a) Jones, C.; Aldridge, S.; Gans-Eichler, T.; Stasch, A. *Dalton Trans.* **2006**, 5357−5361. (b) Evans, D. R.; Mathur, R. S.; Heerwegh, K.; Reed, C. A.; Xie, Z. *Angew. Chem., Int. Ed. Engl.* **1997**, *36*, 1335−1337. (c) Nishijo, J.; Numao, S.; Judai, K.; Nishi, N. *Polyhedron* **2009**, *28*, 1664−1667. (d) O'Toole, M. G.; Bennett, B.; Mashuta, M. S.; Grapperhaus, C. A. *Inorg. Chem.* **2009**, *48*, 2300−2308. (e) Zhou, H.-B.; Wang, H.-S.; Chen, Y.; Xu, Y.-L.; Song, X.-J.; Song, Y.; Zhang, Y.-Q.; You, X.-Z. *Dalton Trans.* **2011**, *40*, 5999−6006.
(17) (a) Hewitt, I. J.; Lan, Y.; Anson, C. E.; Luzon, J.; Sessoli, R.; Powell, A. K. *Chem. Commun.* **2009**, 6765−6767. (b) Habib, F.; Long, J.; Lin, P.-H.; Korobkov, I.; Ungur, L.; Wernsdorfer, W.; Chibotaru, L. F.; Murugesu, M. *Chem. Sci.* **2012**, *3*, 2158−2164. (c) Joarder, B.; Chaudhari, A. K.; Rogez, G.; Ghosh, S. K. *Dalton Trans* **2012**, *41*, 7695−7699.
(18) (a) Nematirad, M.; Gee, W. J.; Langley, S. K.; Chilton, N. F.; Moubaraki, B.; Murray, K. S.; Batten, S. R. *Dalton Trans.* **2012**, *41*, 13711−13715. (b) Chandrasekhar, V.; Das, S.; Dey, A.; Hossain, S.; Sutter, J.-P. *Inorg. Chem.* **2013**, *52*, 11956−11965.
(19) (a) Ishikawa, N.; Iino, T.; Kaizu, Y. *J. Am. Chem. Soc.* **2002**, *124*, 11440−11447. (b) Hutchings, A.-J.; Habib, F.; Holmberg, R. J.; Korobkov, I.; Murugesu, M. *Inorg. Chem.* **2014**, *53*, 2102−2112. (c) Iasco, O.; Novitchi, G.; Jeanneau, E.; Luneau, D. *Inorg. Chem.* **2013**, *52*, 8723−8731.
(20) (a) Langley, S. K.; Moubaraki, B.; Murray, K. S. *Polyhedron* **2013**, *64*, 255−261. (b) Zhang, L.; Zhang, P.; Zhao, L.; Lin, S.-Y.; Xue, S.; Tang, J.; Liu, Z. *Eur. J. Inorg. Chem.* **2013**, 1351−1357. (c) Yan, P.-F.; Lin, P.-H.; Habib, F.; Aharen, T.; Murugesu, M.; Deng, Z.-P.; Li, G.-M.; Sun, W.-B. *Inorg. Chem.* **2011**, *50*, 7059−7065. (d) Alexandropoulos, D. I.; Mukherjee, S.; Papatriantafyllopoulou, C.; Raptopoulou, C. P.; Psycharis, V.; Bekiari, V.; Christou, G.; Stamatatos, T. C. *Inorg. Chem.* **2011**, *50*, 11276−11278.
(21) (a) Habib, F.; Murugesu, M. *Chem. Soc. Rev.* **2013**, *42*, 3278−3288. (b) Lin, P.-H.; Sun, W.-B.; Yu, M.-F.; Li, G.-M.; Yan, P.-F.; Murugesu, M. *Chem. Commun.* **2011**, *47*, 10993−10995. (c) Ren, M.; Bao, S.-S.; Hoshino, N.; Akutagawa, T.; Wang, B.; Ding, Y.-C.; Wei, S.; Zheng, L.-M. *Chem.—Eur. J.* **2013**, *19*, 9619−9628.

DOI: 10.1021/acs.inorgchem.5b00343
Inorg. Chem. 2015, 54, 6195−6202